ACS MATERIALS LETTERS

www.acsmaterialsletters.org

Unraveling Water and Salt Transport in Polyamide with Nuclear Magnetic Resonance Spectroscopy

Mahsa Abbaszadeh,[△] Madeline Garell,[△] Ji Il Choi, Yudan Chen, Johannes Leisen, Seung Soon Jang,* Yan-Yan Hu,* and Marta C. Hatzell*

Cite This: *ACS Materials Lett.* 2023, 5, 291−298

Read Online

ACCESS | Metrics & More | Article Recommendations | Supporting Information

ABSTRACT: **Quantifying water and salt transport properties in polyamide is of growing importance as the use of reverse osmosis membranes grows in many industries. Here, using solid-state nuclear magnetic resonance (NMR) spectroscopy, we measure the translational diffusion coefficients using pulsed-field gradient NMR, examine ion dynamics with NMR relaxometry, and determine the activation energy barriers of hydrogen and sodium ions in ion-exchanged polyamide using variable-temperature NMR. We identify two predominant diffusion components within the spectra associated with bound and unbound hydrogen and sodium ions. We show that the diffusion coefficient of the bound hydrogen ions decreases by ∼50% while the unbound hydrogen diffusion coefficient remains constant as the salinity of the mixture doubles. Conversely, the bound sodium diffusion coefficient remained constant while the unbound sodium diffusion coefficient decreased by ∼40% as the salinity of the mixture doubled. Through examining the spin−lattice relaxation time (T_1) we also report the associated activation energy for sodium and hydrogen. We believe these molecular-scale measurements can aid in extending physics-based models of salt and water transport in high-pressure reverse osmosis applications.**

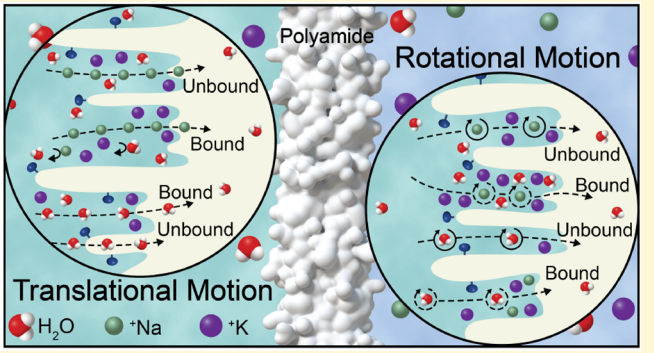

The development of highly permeable thin film composite polyamide membranes with high salt rejection has allowed reverse osmosis (RO) to become the leading technology for seawater and industrial water desalination.[1−4] Commercial RO membranes have an active aromatic polyamide layer which is formed by interfacial polymerization.[5−9] At a macroscale, commercial polyamide RO membranes achieve near ideal salt rejection (>98%), high water permeability (2−20 L m^{-2} h^{-1} bar^{-1}), and low salt permeability (0.1−0.4 L m^{-2} h^{-1}).[7,8,10] This high salt rejection is largely ascribed to the unique nonporous and highly tortuous nature of the polyamide layer.[8]

Water and salt transport properties through polyamide are largely limited to physics extrapolated from the solution-diffusion model.[1,11] For instance, bench-scale measurement of water and salt permeability is commonly used to extract water and salt diffusion coefficients.[7,12,13] While the solution-diffusion model is well tested, the model assumes that chemical and hydraulic gradients are constant, and that all transport processes occur under equilibrium conditions.[12,14−16] These core assumptions of the solution-diffusion model are becoming increasingly limiting as the field moves beyond seawater as the primary feed stream.[14,17−19]

Advanced characterization techniques that aim to extrapolate water and salt transport in membranes include transmission electron microscopy (TEM), quasielastic and inelastic neutron scattering (QENS, INS), extended X-ray absorption fine structure (EXAFS), full-field transmission X-ray microscopy 2D and 3D (TXM-CT and microCT), positron annihilation lifetime spectroscopy (PALS), and nuclear magnetic resonance (NMR) spectroscopy.[20−24] TEM images predict that the average water diffusion coefficient in polyamide is 1.03 ± 0.02−1.67 ± 0.04 × 10^{-9} m^2/s.[21] Quasielastic neutron scattering experiments suggest that the

Received: October 2, 2022
Accepted: December 21, 2022
Published: December 27, 2022

https://doi.org/10.1021/acsmaterialslett.2c00932
ACS Materials Lett. 2023, 5, 291−298

water diffusion coefficient is 1.9 ± 0.4 × 10^{-9} m^2/s.[25] Molecular dynamics simulations of a hydrated polyamide membrane suggest the diffusion coefficient of the bulk phase is 3.08 × 10^{-9} m^2/s, the interface region 0.58 × 10^{-9} m^2/s, and the polyamide membrane 0.24 × 10^{-9} m^2/s.[26] Examining sodium diffusion in polyamide is feasible through pulse field gradient NMR, yet to date there are only a handful of investigations which have been completed.[27−31]

Herein, we have prepared polyamide membranes which are ion-exchanged with different salt mixtures and at different levels of relative humidity (0%, 60%, and 98%). We applied pulsed field gradient (PFG) NMR to examine the translational diffusion coefficients of hydrogen and sodium ions in ion-exchanged polyamide.[32,33] We also measured ^{1}H and ^{23}Na NMR spin−lattice relaxation time (T_1) and extracted the activation energy for salt and water transport for the various conditions.

First, we examine the translational (Figure 1a) and rotational (Figure 1b) motion of water (^{1}H) in fully hydrated polyamide

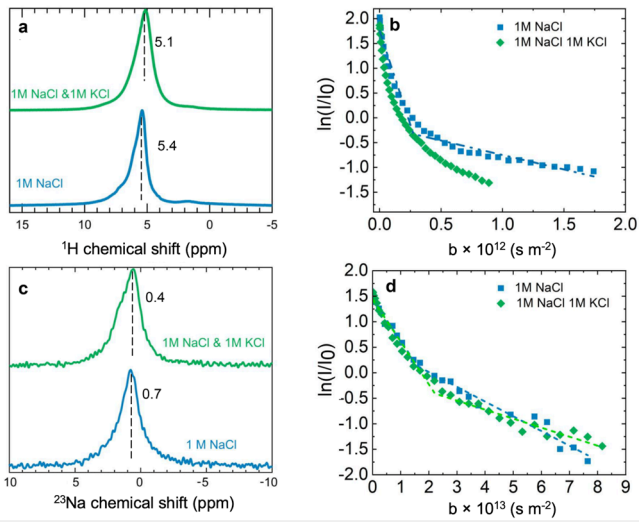

Figure 1. ^{1}H and ^{23}Na NMR for probing local environments and diffusion coefficients. (a) ^{1}H NMR spectra, (b) D_1 and D_2 fitting of ^{1}H PFG NMR decay for hydrogen translational motion (diffusion), (c) ^{23}Na NMR spectra, and (d) D_1 and D_2 fitting of ^{23}Na PFG NMR decay detecting sodium translational motion(diffusion).

as salinity increased from 1 to 2 M using PFG NMR. As the salinity doubled, there was a clear broadening of the ^{1}H line-width spectra (Figure 1a and Figures S1 and S3) indicating that the rotational movements are hindered in the presence of higher salt concentration. When examining chemically and magnetically inequivalent components within the ^{1}H spectra, we identified four peaks. Two peaks follow a 2-component distribution model (~5 ppm). The diffusion coefficients attributed to the peak ~1.3 ppm were unchanged under all conditions and thus were assumed to be ascribed to the polymer functional groups. The second two were ascribed to bound and unbound hydrogen. The two bound and unbound hydrogen diffusion coefficients changed with salinity and were attributed to the ^{1}H resonance around 5 ppm.

When examining the rotational and translational motion of water within polyamide, as the salinity increases from 1 to 2 M (Figure 1a, green line), the unbound hydrogen decreases from ~15% to ~5%, and the amount of bound hydrogen increases from ~82% to ~94% (as determined by deconvolution of line-shapes as shown in Figure S1). When examining the normalized intensity of the ^{1}H as a function of different gradient strengths, we observe a relaxation (Figure 1b) for water at ~4.7 ppm. The Stejskal−Tanner equation allows for the extraction of diffusion coefficients (SI, eq 2). This equation can be manipulated such that the diffusion coefficient is the slope in plots of $\ln(I/I_0)$ vs b where b is a parameter that depends on the experimental conditions and properties of the nucleus under investigation [$b = \gamma^2 g^2 \delta^2 (\Delta - \delta/3)$]. The unbound hydrogen diffusion coefficient (D_1) does not change with salinity (Figure 1b, Table 1). The unbound hydrogen diffusion coefficient is in the range of 4.7 × 10^{-10} to 4.9 × 10^{-10} m^2/s which is lower than the bulk water (self) diffusion coefficient (2.3 × 10^{-9} m^2/s) (Table 1).[34] The values for self-diffusivity of water in polyamide in this work are also lower than the value for self-diffusivity of bulk water (2.5 × 10^{-9} m^2/s at 300 K) reported by quasielastic neutron scattering.[35] Diffusion of unbound hydrogen is not impacted by increases in salinity. This is not surprising as the molar concentration of water (approximately 55 M) is significantly higher than either salt.

The diffusion coefficient of the bound protons decreases from 7.4 × 10^{-11} ± 7 × 10^{-14} to 4.0 × 10^{-11} ± 0.1 × 10^{-12} m^2/s with the addition of 1 M KCl (Figure 1c, Table 1). The diffusion of bound protons decreases by ~50% with the addition of 1 M KCl to a 1 M NaCl feed stream (Figure 1c and Table 1). This is due to the increase of salt within the polyamide, which acts to sterically block the motion of bound protons.[36] It should be noted that the self-diffusion coefficient of water at room temperature is reported to be at 2.8 × 10^{-9} m^2/s.[1] The presence of more than one diffusion coefficient for ^{1}H could be due to strong hindrance of water mobility in the dense polyamide network, as water molecules are diffusing from a local to bulk diffusion pathway. Here, we assume that the bound water is the molecules that are associated by hydrogen bonding to surface functional groups. The binding of water through hydrogen bonding impedes the transport. When salt is added, the bound hydrogen-containing molecules are hindered from interactions with water and/or carboxylic acid functional groups due to the presence of salt. As salinity increases, the space around the bound water region is tighter leading to a decrease in the bound water diffusion coefficient.

Table 1. Diffusion Coefficient Measurements Derived from a PFG Experiment for Fully Hydrated Ion-Exchanged Polyamide

diffusion PFG experiments			
multi-ionic mixture	nucleus	D_1 (unbound) (m^2 s^{-1})	D_2 (bounded) (m^2 s^{-1})
1 M NaCl	^{23}Na	9.4 × 10^{-12} ± 0.5 × 10^{-12}	2 × 10^{-12} ± 0.2 × 10^{-12}
1 M NaCl + 1 M KCl	^{23}Na	5.8 × 10^{-12} ± 0.5 × 10^{-12}	2 × 10^{-12} ± 0.1 × 10^{-12}
1 M NaCl	^{1}H	4.9 × 10^{-10} ± 0.4 × 10^{-12}	7.4 × 10^{-11} ± 7 × 10^{-12}
1 M NaCl + 1 M KCl	^{1}H	4.7 × 10^{-10} ± 0.8 × 10^{-12}	4.0 × 10^{-11} ± 0.1 × 10^{-12}

https://doi.org/10.1021/acsmaterialslett.2c00932
ACS Materials Lett. 2023, 5, 291−298

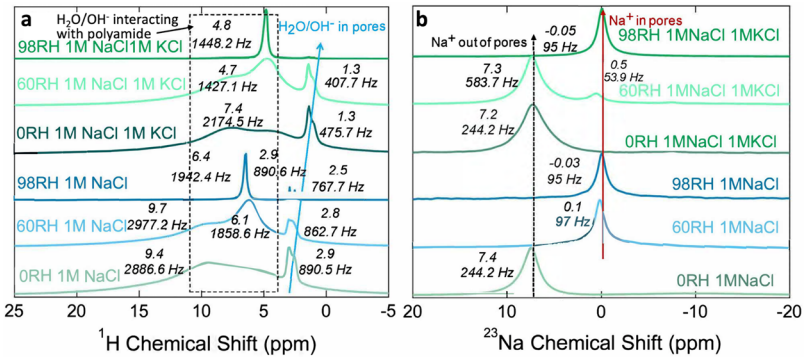

Figure 2. (a) ^{1}H and (b) ^{23}Na MAS NMR spectra of ion-exchanged polyamide at different levels of humidity and ionic mixtures. MAS rate: 10 kHz.

The bound hydrogen diffusion behavior in polyamide is dependent upon interactions with dipoles of carboxylates of polyamide, water−water, water−polymer, water−sodium−potassium, and electrostatic interactions.

Next, we examine the translational (Figure 1d) and rotational (Figure 1c) motion of salt (^{23}Na) in polyamide as salinity increases from 1 to 2 M using PFG NMR. As the salinity doubled, like the ^{1}H spectra, there is a clear broadening of the ^{23}Na line-width spectra (Figure 1c and Figure S2). This indicates that the rotational and translational movements are hindered in the presence of higher salt concentrations. When examining the components within the ^{23}Na spectra, we identified two peaks. The two peaks were ascribed to bound and unbound sodium (Figure 1c and Figure S2). When examining the rotational and translational motion of sodium within the membrane, as the salinity increases from 1 to 2 M, (Figure 1c, green line) the unbound sodium decreases from 90% to 75%, and the amount of bound ions increases from 10% to 25% (as determined by deconvolution of line-shapes as shown in Figure S2). Thus, the hindrance in sodium ion movement is due to the increase in the amount of sodium that exists in the bound state in the presence of high salinity.

When examining the normalized intensity of the ^{23}Na as a function of different gradient strengths, we observe a signal relaxation (Figure 1d). The unbound sodium diffusion decreases by 40% from $9 \times 10^{-12} \pm 0.5 \times 10^{-12}$ to $6 \times 10^{-12} \pm 0.5 \times 10^{-12}$ m^2/s (Figure 1d and Table 1). The decrease in the unbound diffusion coefficient of sodium may be due to the competitive diffusion between sodium and potassium as salinity increases. The bound diffusion coefficient (D_2) does not change as the ionic strength increases and remains around $2 \times 10^{-12} \pm 0.2 \times 10^{-12}$ m^2/s (Figure 1d and Table 1). Our results show that the bound and unbound diffusion coefficients of sodium ions in ion-exchanged polyamide are less than the sodium ion diffusion reported in water ($D_{NaCl} = 1.6 \times 10^{-9}$ m^2/s) by approximately a factor of 100.[37,38] This is due to the fact that there are most likely low concentrations of sodium physiochemically interacting with the polymer as sodium is able to freely move within the free space of the polymer. We deduce that, with an increase in salinity, the translational movements of the unbound sodium ions passing through polyamide are hindered. For unbound sodium ions, the high salinity reduces Brownian motion and provides accessible open space for the translational motions of sodium ions. In this case, sodium ions with a large hydrodynamic radius may encounter more boundaries and thereby travel smaller distances. The ion transport in polymeric membranes is also usually governed by Donnan exclusion, dielectric exclusion, and size exclusion. Since the ion-exchanged polyamide membrane contains the same functional groups with similar charge properties in different ionic mixtures, the PFG NMR diffusometry results suggest that a size-exclusion mechanism dominates the ion translational motions resulting from the dense structure of the polyamide network.[39] Compared to the water diffusion coefficient values obtained by other advanced characterization techniques reported elsewhere,[20−24] our diffusion coefficient values for hydrogen are approximately 10 times smaller (for unbound hydrogen). We hypothesize that the lower diffusion coefficient value obtained in our study is due to measurements for bulk polyamide and not a thin film.

Herein, we used magic angle spinning (MAS) to produce high-resolution NMR spectra to to obtain structural information in the polyamide. MAS NMR spins the sample at the magic angle (54.74°) with respect to the direction of the magnetic field. Using MAS, we can obtain high-resolution data where line-shapes are narrowed due to elimination of dipolar (for 1H) and quadrupolar (for 23Na) interactions.. However, since the MAS in this work is in the range of 10 kHz, we hypothesized that there exists some remaining 1H-1H dipolar and quadrupolar interactions. MAS is a powerful method for analyzing chemical environments at the atomic level.

The peak positions and the line width of the ^{1}H signal vary with changes in relative humidity and salinity (Figure 2a). At low relative humidity (RH = 0%), the physics examined is due only to the properties of the polymer. Ideally, enhanced transport within the polymer itself can allow enhanced transport within the hydrated polymer, which is important to examine. Without hydration, the (H_2O/OH^-) motion is ascribed to hindered movements within the pores, at the membrane interface, and outside the pores (Figure 2a). At low relative humidity, when salinity increases, the peak positions of ^{1}H shift toward lower values (ppm). As ^{1}H shifts toward lower ppm values, we hypothesize that hydrogen peaks are attributed to the bonding of water (hydrogen) with amide functional groups. On the contrary, as the ^{1}H peak shifts toward higher ppm, we hypothesize that water molecules (hydrogen) bond with the carboxylic acid functional groups of polyamide.[40] This is because polyamide is more decorated with linear chains at the interface (carboxylic acid functional groups) and more fully cross-linked aggregates (amide functional groups) in the core part of the polymer.[41] Thus, these interactions can provide some insight on whether water is within the interphase or within a pore.

https://doi.org/10.1021/acsmaterialslett.2c00932
ACS Materials Lett. 2023, 5, 291−298

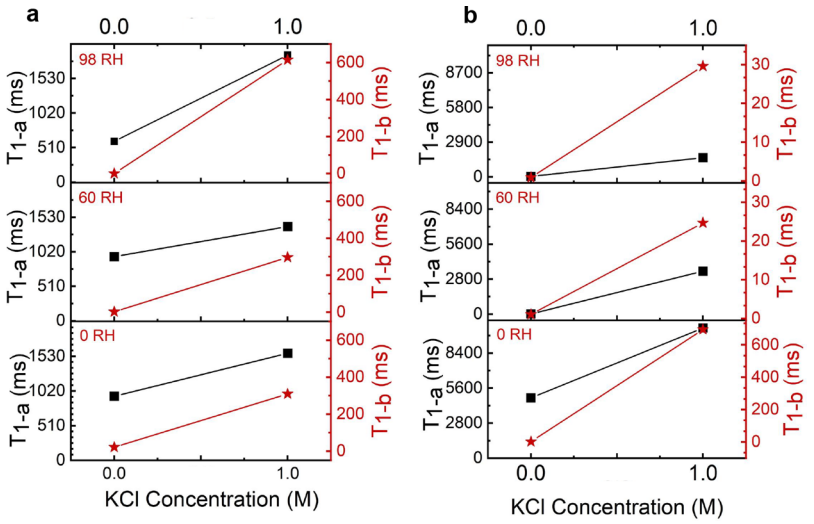

Figure 3. T_{1-a} (component 1, left *y*-axis, black lines with square symbols) and T_{1-b} (component 2, right *y*-axis, red lines with star symbols) for (a) ^{1}H and (b) ^{23}Na NMR of samples with varied concentrations of KCl solution in the ionic mixture. The legend in each graph indicates the relative humidity (RH, %).

At high relative humidity (RH= ∼98%), the physics examined is largely due to polymer−water interactions. With hydration, we observed a sharp peak in the ^{1}H spectra, indicating fast rotational motions of water molecules. Increased molecular mobility is expected because water hydrates the polymer. This phenomenon results in an increased effective magnetic field (higher ppm values), and this effect can be caused by the presence of specific functional groups that withdraw electron density from hydrogen ions, such as amide functional groups in polyamide. This gives us information that the hydrogen ions are closer to amide functional groups as the relative humidity of the membranes increases. However, with high relative humidity, when salinity increases, the ^{1}H spectra shift toward lower ppm by 2.4 ppm (Figure 2a). Furthermore, the signal indicates that the water within the pores vanishes. Therefore, since salt infiltrates the pores, water is displaced to the polyamide interface (Figure S1).

The peak positions (chemical changes) of the sodium signal and the line width of ^{23}Na also vary with changes in relative humidity and salinity (Figure 2b). Without hydration, the Na^{+} movement is attributed to hindered movements outside the pores (Figure 2b). At low relative humidity, when salinity increases, the ^{23}Na shift or line-width does not change significantly.

With hydration (RH = ∼98%), we observed a sharp peak in the ^{23}Na spectra, and a shift in the peak position from ∼7.3 to ∼0. This shows that sodium ions move toward polyamide pores with increasing humidity (Figure 2b). As the sodium peak changes to higher values, the sodium ions interact with the carboxylic acid of polyamide on the surface, since the higher chemical changes for the sodium peaks are usually related to the interaction of sodium with an acidic environment (Figure S5). At higher RH, sodium ions become on average more hydrated, and the distance between sodium ions increases, thus reducing the asymmetry in the surrounding electronic environment.[42] This results in a decrease in electric field gradients (EFGs) in the ^{23}Na nuclei, leading to a reduced quadrupolar broadening.[42]

The parameters of the nuclear spin−lattice relaxation rate (T_1), which accounts for the longitudinal relaxation time, depend on the fluctuation of the nuclear spins of the ions in the range of the larmor frequency (MHz). Therefore, measuring nuclear spin−lattice relaxation rates can provide information on the interaction of molecules with their chemical environments.[43] In an effort to examine the rotational movement of hydrogen and sodium, we performed spin−lattice relaxation experiments.

We observed that spin−lattice relaxation times (T_1) follow a bimodal distribution of ions attributed to the presence of two different environments (biexponential relaxation, two components). This is consistent with our PFG NMR experiments and further confirms that the two-site model for bound and unbound ions is appropriate for the polyamide−salt mixture. Bound ions are located in regions of strong confinement, along with regions where unbound ions coordinate with other hydrated nuclei.

The T_1 relaxation time for the unbound site is indicated as T_{1-b} whereas the T_1 relaxation time for the bound state is indicated as T_{1-a} (Figure 3). For rigid cross-linked polymers, most of the ionic molecular motion near room temperature is in the slow motion region, which means that a longer T_1 suggests slower motion ($T_{1-a} > T_{1-b}$).[5] When we plotted the magnetization intensity as a function of the recovery time for sodium and hydrogen ions in polyamide (Figure S7 and Tables S1 and S2), we observed that the T_1 relaxation for both hydrogen (Figure 3a) and sodium ions (Figure 3b) (bound and unbound) continued to increase with salinity (all levels of RH), suggesting that sodium and hydrogen ionic motions are hindered as the feed stream becomes more concentrated.

For the same salt mixture, as the relative humidity of the polyamide membrane increases, the spin−lattice relaxation time for sodium/hydrogen ions (both bound and unbound) becomes shorter, meaning that the overall motion of the fluid-lattice surrounding the ions increases (Figure 3a,b). It should be noted that the T_1 values for ^{23}Na in polyamide are still higher compared to the relaxation times of ^{23}Na in a dilute NaCl solution (T_1 = 49.6 ms, T_2 = 34.0 ms).[44,45] In summary, the results of relaxation rates for rotational motions of ions follow the same trend as those observed in the study of translational motions derived from diffusion coefficients with respect to varying RH and salinity.

https://doi.org/10.1021/acsmaterialslett.2c00932
ACS Materials Lett. 2023, 5, 291−298

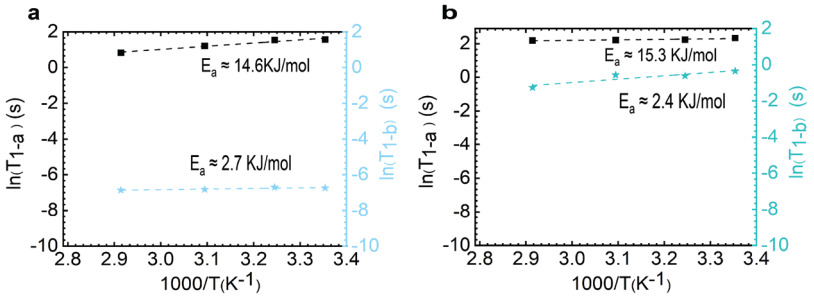

Figure 4. $\ln(T_{1-a})$ (left-axis) and $\ln(T_{1-b})$ (right-axis) of ^{23}Na NMR for ion-exchanged polyamide in (a) 1 M NaCl and (b) 1 M NaCl and 1 M KCl at 0 relative humidity (RH, 0%).

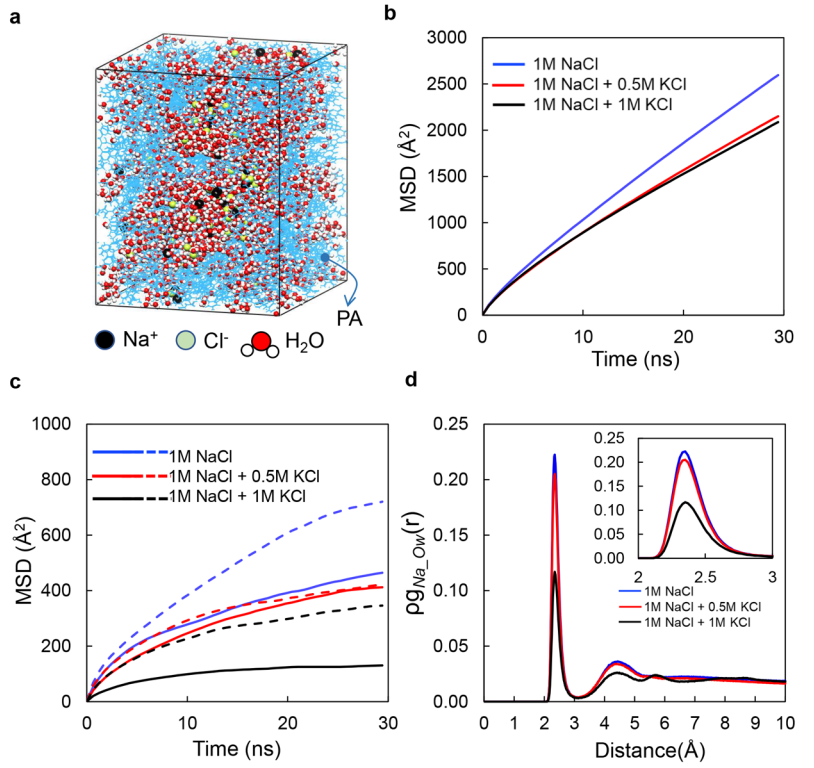

Figure 5. (a) Representative model for cross-linked polyamine membrane with ions solvated in water. The mean square displacement is computed for (b) H_2O and (c) Na^+ and Cl^- ions, where the diffusion of the Cl^- ion is higher than that of Na^+. (d) Pair correlation analysis for the Na^+-O of water pair in which the oxygen of H_2O is denoted by O_w.

We have measured the energy barrier (E_a) of protons and sodium ions due to rotational motions by detecting relaxation times as a function of temperature. The T_1 values were measured at four temperatures of 25, 35, 50, and 70 °C to determine the energy barrier using Arrhenius plots (at RH = 0). Without hydration, the energy barrier is expected to be high because it is the polymer, not the hydrated polymer.

As salinity increases, the activation energy barrier of bound sodium rotational motions in ion-exchanged polyamide increases by 4.8% from 14.6 kJ/mol (1 M) to 15.3 kJ/mol (2 M) (Figure 4. Meanwhile, the unbound sodium ion activation energy barrier shows a 13% decrease with the changes in the ionic mixture. At the molecular level, we know from the PFG experiments that the unbound sodium shifts toward the bound state with increasing salinity. Thus, the observed energy change with the bound state may be due to the relatively higher amount of bound sodium under conditions of low relative humidity (Figure S8).

For hydrogen nuclei, we observe that the relationship for T1 relaxation time versus temperature does not necessarily follow a linear trend (R^2 < 0.9) (Figures S7 and S9). Therefore, we assumed that the dynamics of water in the polyamide remains bound at a very low level of relative humidity (0 RH) and in the presence of other ions (Na^+, K^+, and Cl^-). Therefore, an increase in the temperature of the polyamide environment does not overcome the energy barrier for rotational motions without hydration. We hypothesize that water has more affinity to bind to small ions tightly than binding to other water neighboring molecules,[46] contributing to the bound water remaining bound at higher temperatures or higher concentrations of KCl.

We illustrate a representative computational model in which Na^+ and Cl^- ions are distributed with water (Figure 5a). Our molecular dynamics (MD) simulations were performed using three-dimensional cross-linked polyamide (PA) membrane structures rather than two-dimensional sandwiched PA slab

https://doi.org/10.1021/acsmaterialslett.2c00932
ACS Materials Lett. 2023, 5, 291−298

structures[47] to investigate ion diffusion through the water phase in the PA membrane instead of interfacial ion transport between bulk water and the PA membrane. We carried out all simulations in an isothermal−isobaric (NPT) ensemble under atmospheric pressure conditions of 298.15 K and 1 atm until they reached equilibrium states in terms of density and potential energy fluctuations, as indicated in Figure S11.

The density of the bulk PA structure is determined to be 1.16 and 1.22 g/cm^3 at the dry and hydrated states, respectively. Systems containing ions are found to have slightly higher density. Table S3 summarizes the average density values obtained from the MD simulations for the three systems. It should be noted that all hydrophilic polar functional groups, such as carboxyl and amino groups, and charged species such as Na^+ and Cl^- are solvated by water molecules in the PA membrane. Therefore, we expect the dynamics of ions to be coupled with that of water molecules. Here, we investigate the self-diffusion (D) of ions and water molecules by analyzing the mean square displacement (MSD) calculated as a function of time (t) using eq 1.

$$D = \frac{1}{6}\lim_{t\to\infty}\frac{1}{t}[(r(t) - r(0))^2] \quad (1)$$

Here, $r(0)$ and $r(t)$ denote the position of the particle at the beginning and at time t, respectively, and $[(r(t) - r(0))^2]$ is the mean square displacement (MSD).

We have shown (Figure 5b,c, MSD plots for water) that, for Na^+ and Cl^-, the MSD decreases as the concentration of KCl increases to 1 M, and the slope of the linear segment taken from each MSD curve is found to decrease accordingly. These results indicate that the diffusivities of water and ions are reduced with increasing KCl concentration, as summarized in Table S3. The diffusivity of Cl^- is found to be higher than that of Na^+, which is attributed to the more electrostrict character of water molecules adjacent to the cation compared to the anion of the same charge.[48] Overall, the diffusion of water is on is an order of magnitude higher than the diffusion of ions, because the ions in weakly solvated states tend to be associated with surrounding chemical species of PA such as functional groups or neighboring ions via clustering or aggregation for further stabilization, which diminishes the mobility of ions. Therefore, lower diffusion coefficients are expected, especially for the Na^+ ion.

In this paper, we implement pair-correlation analysis between the Na^+ ions and solvating water molecules. We show that the correlation of Na^+ with water molecules decreases as the KCl concentration increases (Figure 5d). Thus, it is evident that the presence of KCl weakens the solvation state of the Na^+ ion and thereby decreases the Na^+ diffusivity, which emphasizes the sensitivity of the ion mobility in the PA membrane to the local solvation environment.

Here, we used solid-state nuclear magnetic resonance (NMR) spectroscopy to examine the transport of water and salt in polyamide. We investigated the dynamics of H^+ and Na^+ ions at different levels of relative humidity in various high-salinity environments. We identified that water and sodium exist in both "bound" and "unbound" states within the polyamide. These species are attributed to highly immobile "bound" sodium/hydrogen and a more mobile "unbound" sodium/hydrogen. These states are confirmed in both PFG and nuclear spin−lattice relaxation NMR experiments, and with molecular dynamics simulations. In addition, we report the diffusion coefficients for both bound and unbound sodium and water states in the polyamide. NMR spin−lattice relaxation T_1 showed that T_1 decreases with temperature, concluding that spin−lattice relaxation obeys the Arrhenius relation. The activation energy for sodium also showed an increase in the unhydrated polymer with increasing salinity, which was consistent with the PFG diffusion experiments.

■ ASSOCIATED CONTENT

Supporting Information

The Supporting Information is available free of charge at https://pubs.acs.org/doi/10.1021/acsmaterialslett.2c00932.

Materials and methods, computational details, supporting data including NMR 1-D spectra deconvolution, PFG signal intensity decay, static ^{23}Na NMR spectra, T_1 components of ^{1}H nuclei, tables of ^{23}Na and ^{1}H T_1 components, spin−lattice relaxation of ^{23}Na and ^{1}H, density and potential energy fluctuation profiles, diffusion coefficients, ^{1}H SOLA deconvolution of ssNMR spectra, and ^{13}C CP/MAS spectrum of polyamide (PDF)

■ AUTHOR INFORMATION

Corresponding Authors

Seung Soon Jang − *School of Materials Science and Engineering, Georgia Institute of Technology, Atlanta, Georgia 30332, United States;* orcid.org/0000-0002-1920-421X; Email: seungsoon.jang@mse.gatech.edu

Yan-Yan Hu − *Department of Chemistry and Biochemistry, Florida State University, Tallahassee, Florida 32306, United States; Center of Interdisciplinary Magnetic Resonance, National High Magnetic Field Laboratory, Tallahassee, Florida 32310, United States*; Email: yhu@fsu.edu

Marta C. Hatzell − *George W. Woodruff School of Mechanical Engineering, Georgia Institute of Technology, Atlanta, Georgia 30332, United States; School of Chemical and Biomolecular Engineering, Georgia Institute of Technology, Atlanta, Georgia 30332, United States;* orcid.org/0000-0002-5144-4969; Email: marta.hatzell@me.gatech.edu

Authors

Mahsa Abbaszadeh − *George W. Woodruff School of Mechanical Engineering, Georgia Institute of Technology, Atlanta, Georgia 30332, United States*

Madeline Garell − *George W. Woodruff School of Mechanical Engineering, Georgia Institute of Technology, Atlanta, Georgia 30332, United States*

Ji Il Choi − *School of Materials Science and Engineering, Georgia Institute of Technology, Atlanta, Georgia 30332, United States*

Yudan Chen − *Department of Chemistry and Biochemistry, Florida State University, Tallahassee, Florida 32306, United States*

Johannes Leisen − *School of Chemistry and Biochemistry, Georgia Institute of Technology, Atlanta, Georgia 30332, United States*

Complete contact information is available at: https://pubs.acs.org/10.1021/acsmaterialslett.2c00932

Author Contributions

△M.A. and M.G. are co-first authors, each contributed equally. CRediT: **Madeline Garell** data curation, formal analysis, investigation, methodology, writing-original draft, writing-

https://doi.org/10.1021/acsmaterialslett.2c00932
ACS Materials Lett. 2023, 5, 291−298

review & editing; **Ji Il Choi** data curation, formal analysis, visualization; **Yudan Chen** data curation, formal analysis, methodology; **Johannes Leisen** resources, software, supervision, validation; .

Author Contributions

CRediT: **Mahsa Abbaszadeh** data curation, formal analysis, methodology, writing-original draft, writing-review & editing; **Madeline Garell** data curation, formal analysis, investigation, methodology, writing-original draft, writing-review & editing; **Ji Il Choi** data curation, formal analysis, visualization; **Yudan Chen** data curation, formal analysis, methodology; **Johannes Leisen** resources, software, supervision, validation; **Seung Soon Jang** investigation, project administration, software, writing-review & editing; **Yan-Yan Hu** investigation, methodology, project administration; **Marta C. Hatzell** conceptualization, data curation, formal analysis, funding acquisition, methodology, project administration, resources, supervision, visualization, writing-original draft, writing-review & editing.

Notes

The authors declare no competing financial interest.

■ ACKNOWLEDGMENTS

The authors acknowledge the Office of Naval Research (N00014-20-12559). Y.-Y.H. and Y.C. acknowledge the support from National Science Foundation under Grant no. DMR-1847038

■ REFERENCES

(1) Geise, G. M.; Park, H. B.; Sagle, A. C.; Freeman, B. D.; McGrath, J. E. Water permeability and water/salt selectivity tradeoff in polymers for desalination. *J. Membr. Sci.* **2011**, *369*, 130−138.

(2) Epsztein, R.; DuChanois, R. M.; Ritt, C. L.; Noy, A.; Elimelech, M. Towards single-species selectivity of membranes with subnanometre pores. *Nat. Nanotechnol.* **2020**, *15*, 426−436.

(3) Liu, G.; Zhang, X.; Di Yuan, Y.; Yuan, H.; Li, N.; Ying, Y.; Peh, S. B.; Wang, Y.; Cheng, Y.; Cai, Y.; Gu, Z.; Cai, H.; Zhao, D. Thin-film nanocomposite membranes containing water-stable zirconium metal−organic cages for desalination. *ACS Materials Letters* **2021**, *3*, 268−274.

(4) Guo, Y.; Yu, G. Materials Innovation for Global Water Sustainability. *ACS Materials Letters* **2022**, *4*, 713−714.

(5) Kwak, S.-Y.; Woo Ihm, D. Use of atomic force microscopy and solid-state NMR spectroscopy to characterize structure-property-performance correlation in high-flux reverse osmosis (RO) membranes. *J. Membr. Sci.* **1999**, *158*, 143−153.

(6) Abbaszadeh, M.; Krizak, D.; Kundu, S. Layer-by-layer assembly of graphene oxide nanoplatelets embedded desalination membranes with improved chlorine resistance. *Desalination* **2019**, *470*, 114116.

(7) Wang, L.; Cao, T.; Dykstra, J. E.; Porada, S.; Biesheuvel, P. M.; Elimelech, M. Salt and Water Transport in Reverse Osmosis Membranes: Beyond the Solution-Diffusion Model. *Environ. Sci. Technol.* **2021**, *55*, 16665−16675.

(8) Ritt, C. L.; Stassin, T.; Davenport, D. M.; DuChanois, R. M.; Nulens, I.; Yang, Z.; Ben-Zvi, A.; Segev-Mark, N.; Elimelech, M.; Tang, C. Y.; Ramon, G. Z.; Vankelecom, I. F. J.; Verbeke, R. The open membrane database: Synthesis−structure−performance relationships of reverse osmosis membranes. *J. Membr. Sci.* **2022**, *641*, 119927.

(9) Corcos, A. R.; Levato, G. A.; Jiang, Z.; Evans, A. M.; Livingston, A. G.; Mariñas, B. J.; Dichtel, W. R. Reducing the pore size of covalent organic frameworks in thin-film composite membranes enhances solute rejection. *ACS Materials Letters* **2019**, *1*, 440−446.

(10) Li, D.; Wang, H. Recent developments in reverse osmosis desalination membranes. *J. Mater. Chem.* **2010**, *20*, 4551−4566.

(11) Paul, D. R. The Solution-Diffusion Model for Swollen Membranes. *Separation and Purification Methods* **1976**, *5*, 33−50.

(12) Wijmans, J. G.; Baker, R. W. The solution-diffusion model: a review. *J. Membr. Sci.* **1995**, *107*, 1−21.

(13) Verliefde, A. R. D.; Van der Meeren, P.; Van der Bruggen, B.Solution-Diffusion Processes. In *Encyclopedia of Membrane Science and Technology*; John Wiley & Sons, Ltd, 2013; pp 1−26.

(14) Biesheuvel, P. M.; Zhang, L.; Gasquet, P.; Blankert, B.; Elimelech, M.; van der Meer, W. G. J. Ion Selectivity in Brackish Water Desalination by Reverse Osmosis: Theory, Measurements, and Implications. *Environ. Sci. Technol. Lett.* **2020**, *7*, 42−47.

(15) Shefer, I.; Peer-Haim, O.; Leifman, O.; Epsztein, R. Enthalpic and Entropic Selectivity of Water and Small Ions in Polyamide Membranes. *Environ. Sci. Technol.* **2021**, *55*, 14863−14875.

(16) Reif, B.; Ashbrook, S. E.; Emsley, L.; Hong, M. Solid-state NMR spectroscopy. *Nat. Rev. Methods Primers* **2021**, *1*, 1−23.

(17) Wang, R.; Lin, S. Pore model for nanofiltration: History, theoretical framework, key predictions, limitations, and prospects. *J. Membr. Sci.* **2021**, *620*, 118809.

(18) Hegde, V. H.; Doherty, M. F.; Squires, T. M. A two-phase model that unifies and extends the classical models of membrane transport. *Science* **2022**, *377*, 186−191.

(19) Shaffer, D. L.; Arias Chavez, L. H.; Ben-Sasson, M.; Romero-Vargas Castrillón, S.; Yip, N. Y.; Elimelech, M. Desalination and Reuse of High-Salinity Shale Gas Produced Water: Drivers, Technologies, and Future Directions. *Environ. Sci. Technol.* **2013**, *47*, 9569−9583.

(20) Bone, S. E.; Steinrück, H.-G.; Toney, M. F. Advanced Characterization in Clean Water Technologies. *Joule* **2020**, *4*, 1637−1659.

(21) Culp, T. E.; Khara, B.; Brickey, K. P.; Geitner, M.; Zimudzi, T. J.; Wilbur, J. D.; Jons, S. D.; Roy, A.; Paul, M.; Ganapathysubramanian, B.; Zydney, A. L.; Kumar, M.; Gomez, E. D. Nanoscale control of internal inhomogeneity enhances water transport in desalination membranes. *Science* **2021**, *371*, 72−75.

(22) Pate, S. G.; Xu, H.; O'Brien, C. P. Operando observation of CO 2 transport intermediates in polyvinylamine facilitated transport membranes, and the role of water in the formation of intermediates, using transmission FTIR spectroscopy. *Journal of Materials Chemistry A* **2022**, *10*, 4418−4427.

(23) Hatzell, M. C.; Turhan, A.; Kim, S.; Hussey, D. S.; Jacobson, D. L.; Mench, M. M. Quantification of Temperature Driven Flow in a Polymer Electrolyte Fuel Cell Using High-Resolution Neutron Radiography. *J. Electrochem. Soc.* **2011**, *158*, B717.

(24) Foglia, F.; Frick, B.; Nania, M.; Livingston, A. G.; Cabral, J. T. Multimodal confined water dynamics in reverse osmosis polyamide membranes. *Nat. Commun.* **2022**, *13*, 1−11.

(25) Sharma, V. K.; Singh, P. S.; Gautam, S.; Maheshwari, P.; Dutta, D.; Mukhopadhyay, R. Dynamics of water sorbed in reverse osmosis polyamide membrane. *J. Membr. Sci.* **2009**, *326*, 667−671.

(26) Zhang, N.; Chen, S.; Yang, B.; Huo, J.; Zhang, X.; Bao, J.; Ruan, X.; He, G. Effect of Hydrogen-Bonding Interaction on the Arrangement and Dynamics of Water Confined in a Polyamide Membrane: A Molecular Dynamics Simulation. *J. Phys. Chem. B* **2018**, *122*, 4719−4728.

(27) Xu, X.; Kirkpatrick, R. J. NaCl interaction with interfacially polymerized polyamide films of reverse osmosis membranes: A solid-state 23Na NMR study. *J. Membr. Sci.* **2006**, *280*, 226−233.

(28) Nieuwendaal, R. C.; Wilbur, J. D.; Welsh, D.; Witherspoon, V.; Stafford, C. M. A method to quantify composition, purity, and cross-link density of the active polyamide layer in reverse osmosis composite membranes using 13C cross polarization magic angle spinning nuclear magnetic resonance spectroscopy. *J. Membr. Sci.* **2022**, *648*, 120346.

(29) Kwak, S.-Y. Relationship of relaxation property to reverse osmosis permeability in aromatic polyamide thin-film-composite membranes. *Polymer* **1999**, *40*, 6361−6368.

(30) Stepišnik, J.; Fritzinger, B.; Scheler, U.; Mohorič, A. Self-diffusion in nanopores studied by the NMR pulse gradient spin echo. *EPL (Europhysics Letters)* **2012**, *98*, 57009.

(31) Sagidullin, A.; Meier-Haack, J.; Scheler, U. Molecular mobility and transport in polymer membranes and polyelectrolyte multilayers. *Magn. Reson. Imaging* **2007**, *25*, 541−543.
(32) Callaghan, P. T.*Translational Dynamics and Magnetic Resonance: Principles of Pulsed Gradient Spin Echo NMR*; Oxford University Press, 2011; p 576.
(33) Arges, C. G.; Ramani, V. Two-dimensional NMR spectroscopy reveals cation-triggered backbone degradation in polysulfone-based anion exchange membranes. *Proc. Natl. Acad. Sci. U. S. A.* **2013**, *110*, 2490−2495.
(34) Sharma, V. K.; Singh, P. S.; Gautam, S.; Mitra, S.; Mukhopadhyay, R. Diffusion of water in nanoporous NF polyamide membrane. *Chem. Phys. Lett.* **2009**, *478*, 56−60.
(35) Muscatello, J.; Müller, E. A.; Mostofi, A. A.; Sutton, A. P. Multiscale molecular simulations of the formation and structure of polyamide membranes created by interfacial polymerization. *J. Membr. Sci.* **2017**, *527*, 180−190.
(36) Anderson, J. L.; Quinn, J. A. Restricted Transport in Small Pores: A Model for Steric Exclusion and Hindered Particle Motion. *Biophys. J.* **1974**, *14*, 130−150.
(37) Peeters, J. M. M.; Boom, J. P.; Mulder, M. H. V.; Strathmann, H. Retention measurements of nanofiltration membranes with electrolyte solutions. *J. Membr. Sci.* **1998**, *145*, 199−209.
(38) Bouazizi, S.; Nasr, S. Self-diffusion coefficients and orientational correlation times in aqueous NaCl solutions: Complementarity with structural investigations. *J. Mol. Liq.* **2011**, *162*, 78−83.
(39) Tan, R.; et al. Hydrophilic microporous membranes for selective ion separation and flow-battery energy storage. *Nat. Mater.* **2020**, *19*, 195−202.
(40) Abragam, A.*The Principles of Nuclear Magnetism*; Clarendon Press, 1961; p 666.
(41) Cahill, D. G.; Freger, V.; Kwak, S.-Y. Microscopy and Microanalysis of Reverse-Osmosis and Nanofiltration Membranes. *MRS Bull.* **2008**, *33*, 27−32.
(42) Chen, Y.; Lingwood, M. D.; Goswami, M.; Kidd, B. E.; Hernandez, J. J.; Rosenthal, M.; Ivanov, D. A.; Perlich, J.; Zhang, H.; Zhu, X.; Möller, M.; Madsen, L. A. Humidity-Modulated Phase Control and Nanoscopic Transport in Supramolecular Assemblies. *J. Phys. Chem. B* **2014**, *118*, 3207−3217.
(43) Yan, L.; Hu, Y.; Zhang, X.; Yue, B.Applications of NMR Techniques in the Development and Operation of Proton Exchange Membrane Fuel Cells. In *Annu. Rep. NMR Spectrosc.*; Webb, G. A., Ed.; Academic Press, 2016; Vol. *88*, Chapter 3, pp 149−213.
(44) Guo, X.; Theissen, S.; Claussen, J.; Hildebrand, V.; Kamphus, J.; Wilhelm, M.; Luy, B.; Guthausen, G. Dynamics of Sodium Ions and Water in Swollen Superabsorbent Hydrogels as Studied by 23Na- and 1H-NMR. *Macromol. Chem. Phys.* **2019**, *220*, 1800350.
(45) Engelke, S.; Marbella, L. E.; Trease, N. M.; De Volder, M.; Grey, C. P. Three-dimensional pulsed field gradient NMR measurements of self-diffusion in anisotropic materials for energy storage applications. *Phys. Chem. Chem. Phys.* **2019**, *21*, 4538−4546.
(46) Hribar, B.; Southall, N. T.; Vlachy, V.; Dill, K. A. How Ions Affect the Structure of Water. *J. Am. Chem. Soc.* **2002**, *124*, 12302−12311.
(47) Ding, M.; Szymczyk, A.; Ghoufi, A. Hydration of a polyamide reverse-osmosis membrane. *J. Membr. Sci.* **2016**, *501*, 248−253.
(48) Vitagliano, V.; Lyons, P. A. Diffusion coefficients for aqueous solutions of sodium chloride and barium chloride. *J. Am. Chem. Soc.* **1956**, *78*, 1549−1552.

https://doi.org/10.1021/acsmaterialslett.2c00932
ACS Materials Lett. 2023, 5, 291−298